Pedestal Turbulence Dynamics in ELMing and ELM-free H-mode Plasmas

Z. Yan 1), G.R. McKee 1), R.J. Groebner 2), P.B. Snyder 2), T.H. Osborne 2), M.N.A. Beurskens 3), K.H. Burrell 2), T.E. Evans 2), R.A. Moyer 4), H. Reimerdes 5), and X. Xu 6)

1) University of Wisconsin-Madison, Madison, Wisconsin 53706-1687, USA
2) General Atomics, P.O. Box 85608, San Diego, California 92186-5608, USA
3) EURATOM/CCFE Fusion Association, Culham Sci. Centre, Abingdon, UK
4) University of California-San Diego, La Jolla, California 92121, USA
5) Columbia University, New York, New York, USA
6) Lawrence Livermore National Laboratory, Livermore, California, 94550, USA.

Email contact of main author: yanz@fusion.gat.com

Abstract. Measurements of long wavelength density fluctuations in the pedestal region of DIII-D plasmas have revealed several important features of edge instabilities during type I edge localized mode (ELMing) and ELM-free discharges. These features, measured with a 2D array of beam emission spectroscopy channels, include: toroidal field and spatial dependence of two distinct frequency bands (50–150 kHz and 200–400 kHz) of density fluctuations modulated with the ELM cycle; the low frequency band (50–150 kHz) has dynamics correlated with that of the pedestal electron pressure. High frequency coherent modes observed during quiescent H-mode plasmas exhibit long poloidal scale length, short decorrelation times of a few μs and mode frequency close to ion diamagnetic frequency, qualitatively similar to characteristics expected for kinetic ballooning modes. Core turbulence increases dramatically in plasmas for which ELMs are stabilized via application of an n=3 resonant magnetic perturbation. These observations provide key insights into the underlying turbulence and instability properties that limit pedestal height and width, and will help develop a predictive model for pedestal.

1. Introduction

High confinement (H-mode) plasmas with a spontaneously generated edge transport barrier (pedestal) are of great significance for the performance of future burning plasma device. Core confinement is closely correlated with the pressure on the top of the pedestal (pedestal height). For decades, theories and experiments have been focused on studies of the formation of the pedestal structure and understanding the underlying instabilities. A recently developed model, EPED1 [1], which is based on the hypothesis that the pedestal height is limited by the peeling-ballooning instability and the pedestal width is constrained by the kinetic ballooning mode (KBM) has successfully predicted the pedestal height and width in several experiments [2]. However, experimental tests of the instabilities underlying this theory are still lacking. Characterizing the underlying turbulence and comparing with theory is thus very important to validating theory of pedestal instabilities and ultimately obtaining an accurate predictive model for the pedestal structure.

H-mode pedestals are usually characterized by the presence of the edge localized modes (ELMs), which pose a significant material erosion risk in burning plasma devices. The observation of the suppression of the ELMs by resonant magnetic perturbations (RMP) is hence of great significance [3]. However, the underlying physics is still not well understood: plasma density and rotation typically drop during RMP, and energy confinement may be adversely affected. Detailed documentation of the turbulence characteristics in the edge and core during the RMP is providing new insights and understanding into the underlying physics of ELM suppression via resonant radial magnetic fields.

2. Turbulence Characteristics in the ELMing H-mode Pedestal

Long wavelength density fluctuations are measured using a 2D array of beam emission spectroscopy (BES) channels [4] deployed at $0.9<r/a<1$ during a ρ* ($\rho^* \sim m_i^{1/2} T_i^{1/2}/aB_T$) scan ($\rho^*=\rho_I/a\sim0.4\%$ to 0.8% at pedestal top) on the DIII-D tokamak while the other non-

dimensional parameters, β, ν*, Mach number and T_i/T_e are held constant at the pedestal top [5]. Cross spectrum and cross phase between the poloidally separated BES channels are shown in Fig. 1 as a function of time after an ELM in the Type-I ELMing phase of a typical H-mode plasma for three different ρ* values at r/a~0.95. The data was averaged over hundreds of inter-ELM windows to provide a statistical ensemble average. As is shown in Fig. 1, two distinct bands of density fluctuations, a lower frequency band at 50 kHz to 150 kHz and a higher frequency band at 200 kHz to 400 kHz, are observed and found to propagate in opposite poloidal directions (indicated by the opposite cross phase) in the lab frame at low ρ*. The integrated relative density fluctuation amplitude ($\tilde{n}/n$) over 50 kHz to 400 kHz is a few percent, which is significantly lower than the typical edge fluctuation amplitudes in L mode plasmas ($\tilde{n}/n$~10%). The wave number estimated from the cross phase is $k_\theta\rho_i$~0.08 for the low frequency band mode and $k_\theta\rho_i$~0.17 for the high frequency band at r/a~0.95 at B_T = -2.1 T. Comparing the poloidal turbulence velocity calculated from the time-delay cross correlation between BES channels with the local $E\times B$ velocity measured with charge exchange recombination (CER) system shows the low frequency band is propagating in the ion diamagnetic direction while the high frequency band propagates in the electron diamagnetic direction in the *plasma* frame (where E_r=0). The turbulence decorrelation rate for the low frequency band exceeds equilibrium $E\times B$ shearing rate. The above features observed for the low frequency band are qualitatively similar with that predicted for the KBM. These two-band structures are more prominent at low ρ*. They are modulated with the ELM cycle: mode amplitudes rise monotonically between ELMs and crash at the ELM. A comparison of the mode amplitude at different radial locations shows the modes are limited to the region of maximum pedestal electron pressure gradient.

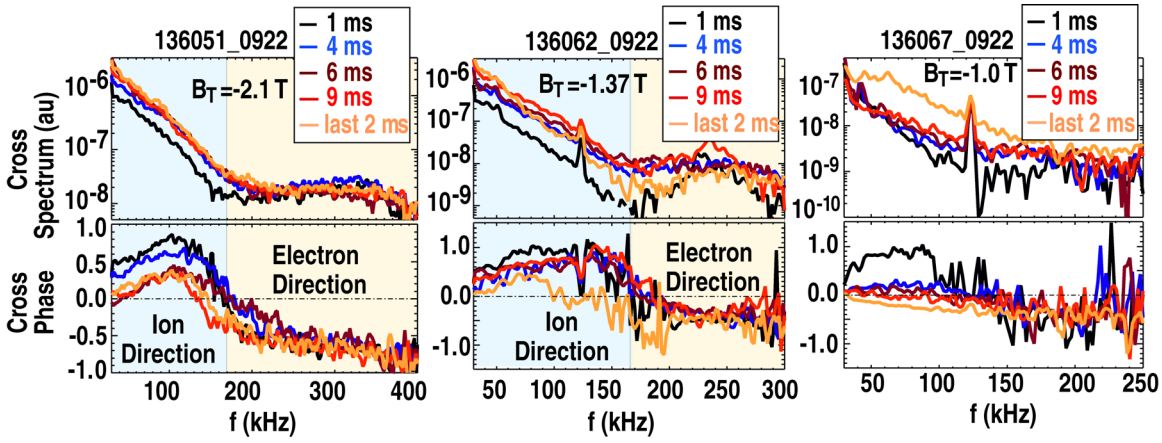

FIG. 1. Pedestal density fluctuation cross spectrum and cross phase (ΔZ = 1.2 cm) for different times relative to an ELM crash at three values of toroidal field (i.e., different ρ) at r/a~0.95. Different colors correspond to different time after an ELM crash.*

In Fig. 1, different colors correspond to different times after an ELM crash. It is observed that at low ρ* (ρ*~0.4%, B_T = -2.1 T), the low frequency band density fluctuation amplitude saturates relatively quickly, within a few ms after an ELM crash. At higher ρ*, it saturates more slowly in ~10 ms. The high frequency band density fluctuation amplitude is observed to be quasi-stationary and does not change significantly with time. This is seen more clearly by integrating the density fluctuations over frequency. Figure 2 is the integrated fluctuation saturation percentage $[(\tilde{n}/n)/(\tilde{n}/n)|_{max}$, $\tilde{n}/n|_{max}$≈1.3%)] as a function of time after an ELM crash at ρ*~0.4%. The diamond symbols are density fluctuation amplitudes from BES measurements integrated over 50 kHz to 150 kHz. The averaged length of the ELM-free window in this plasma is about 17–20 ms. It is interesting to see from the figure that there are two time scales in the evolution of the density fluctuations. First, there is a fast increase of the density fluctuation amplitude that saturates quickly within the first a few ms. Then, the

evolution slows significantly with the fluctuations staying quasi-stationary before the onset of the next ELM. An interesting question is how the dynamics of the density fluctuations are related to the pedestal pressure evolution. The edge pedestal profile is obtained from the standard tanh fits [6]. The time evolution of the pedestal electron pressure after an ELM crash at the pedestal top is shown by the star symbols in Fig. 2. Interestingly, the pedestal electron pressure time evolution is qualitatively similar to the time evolution of the density fluctuation amplitude. This correlation suggests an interaction and coupling between the fluctuations and the profiles. It appears that the fluctuations are generated from the profile gradient and act in turn to limit and saturate the profiles and slow down further gradient increase before the onset of the next ELM.

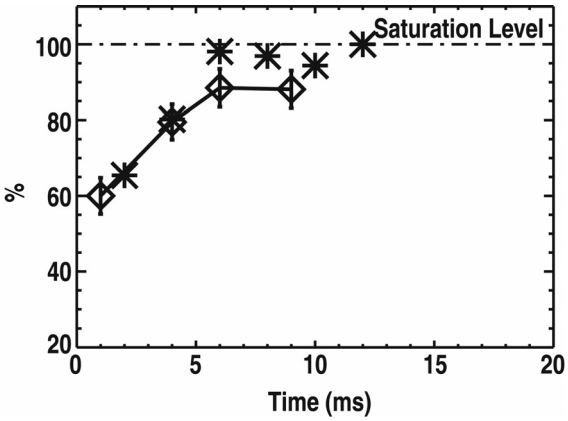

FIG. 2. Density fluctuation amplitude saturated percentage as a function of time after an ELM crash for three different ρ. The ◊ symbols are integrated density fluctuation amplitude over 50 kHz to 150 kHz from BES measurements. The * symbols are pedestal electron pressure time evolution after an ELM crash.*

3. High Frequency Coherent Modes in a Strongly Shaped Quiescent-H mode Plasma

Related experiments were carried out on DIII-D tokamak with a goal of reaching very high pedestal pressure in an ELM-free discharge. High pedestal plasma performance is sought using a highly shaped (high triangularity) plasma [7]. It starts as a standard low density, quiescent-H (QH) mode [8] with a strongly shaped double-null discharge. Once a quasi-steady QH plasma was developed, plasma pedestal density was increased to increase the pedestal pressure and achieve the high performance regime. The 5x6 2D array of BES channels is located at the pedestal region to measure long wavelength density fluctuations. In addition, a 32 channel linear radial array of BES channels is deployed from $0.3<\psi<0.9$ (ψ is normalized poloidal flux).

Figure 3 (a) is a time and frequency resolved density fluctuation spectrogram from BES measurements at $\psi\sim0.95$. Figure 3(b,c) are time varying pedestal electron pressure and D_α light emission respectively. It shows that the edge harmonic oscillation (EHO), which peaks near 15 kHz and is typically observed in the QH discharge, dominates the early time before 2900 ms [Fig. 3(a)] with several harmonics. The EHO is thought to be a low-*n* saturated kink/peeling mode [9]. As the pedestal pressure is increased with increasing pedestal density [Fig. 3(b)], a set of high frequency coherent (HFC) modes peaking around 150 kHz with a uniform frequency separation of ~8 kHz appears in the time window of 3000–4000 ms [Fig. 3(a)]. The EHO disappears as these HFC modes appear. It is also observed from Fig. 3(b) that the pedestal pressure stops increasing with the appearance of the HFC modes, suggesting that they act to saturate the pedestal electron pressure. There are a few discrete ELM events [Fig.3(c)] during this time window, and it is seen that the ELM-like events temporarily reduce the HFC mode amplitude and the pedestal pressure. Between these widely spaced ELMs, HFC modes grow up rapidly with the increasing pedestal pressure. That the individual modes persist on very long time scales (~1 s) and are closely spaced spectrally, yet are well resolved and highly coherent, indicates that the underlying instability is not so strongly driven into a fully turbulent state; this is in contrast to the fluctuations discussed in Sec. 2 in the pedestal of an ELMing H-mode that appear fully turbulent. This is also consistent with the observation that the decorrelation rate of the mode is comparable to or exceeds the high local $E\times B$ shearing rate.

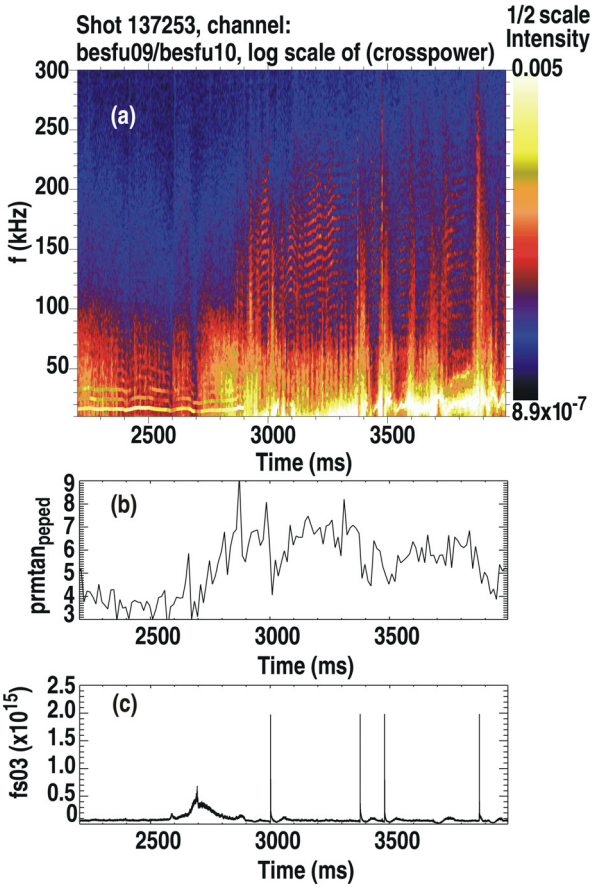

FIG. 3. (a) Cross spectrum between two poloidally separated BES channels showing HFC from ~100–250 kHz starting from time ~2900 ms to 4000 ms; (b) electron pedestal pressure; (c) edge D_α light.

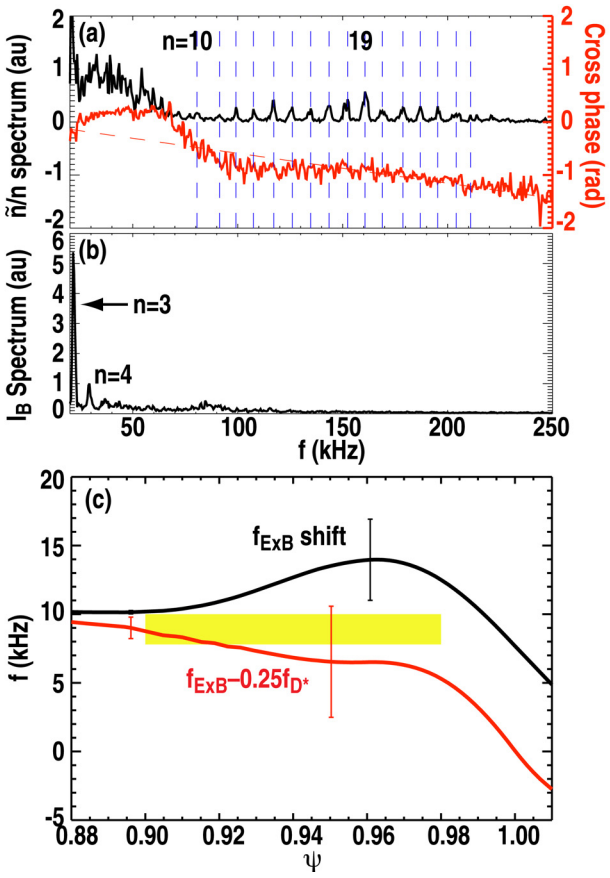

FIG. 4. (a) Relative density fluctuation poloidal cross spectrum (black solid line) and cross phase (red solid line) from BES measurements at ψ~0.95. The red dashed line is a linear fit of the cross phase at frequency between 60 kHz and 250 kHz; (b) magnetic spectrum from edge magnetic probe measurements; (c) E×B rotation frequency (black line), E×B rotation frequency minus a quarter of the ion diamagnetic frequency (red line) and the frequency spacing between successive modes from BES measurements shown by the yellow band.

The cross spectrum between two poloidally separated BES channels from 3200–3220 ms averaged over different poloidal pairs of BES array at the same radial location is computed and shown in Fig. 4. In Fig. 4(a) the black solid line shows the spectrum at the location of ψ~0.95. A broadband turbulence feature is observed below 70 kHz. In the frequency range of 80 kHz and 220 kHz the set of high frequency coherent modes with uniform frequency separation close to 8 kHz is clearly observed. Figure 4(b) is the spectrum of the edge magnetic probes measuring magnetic field fluctuations at an earlier time around 2700 ms when the EHO is dominant. It shows n=3 and n=4 modes at a frequency below 50 kHz. These modes disappear at later time when HFC modes become dominant. The HFC modes seen later are not observed on the magnetic probe measurements. This may result from the low-sensitivity of the probes to the shorter poloidal wavelength of these higher-frequency modes. Based on the wave number analysis compared with ELITE calculations of ballooning mode structures [10], the toroidal mode number of the HFC is estimated from the mode frequency separation, indicated by the blue dashed line in Fig. 4(a). The dominant toroidal mode number is n~19. The safety factor, q_{95} is about 5.5, yielding poloidal mode numbers m~55–104 for the spectra shown. This is consistent with the measured poloidal wavelength

at the outboard midplane, obtained from the cross-phase measurements of poloidally-separated BES channels.

The mode frequency in the plasma frame is found to be close to the 0.2–0.3 times the local ion-diamagnetic frequency. Both the toroidal velocity profiles and the ion temperature profiles are measured by the CER system. The deuterium ion diamagnetic frequency, $f_{D^+} = (dP_{D^+} / d\Psi) / (e \cdot n_{D^+})$, where P_{D^+} and n_{D^+} are deuterium ion pressure and density respectively. In Fig. 4(c) the black solid line is the total $E\times B$ rotation frequency, $f_{E\times B}=k_\theta \cdot V_{E\times B}$. The $E\times B$ velocity is in the electron diamagnetic direction in the lab frame. The red solid line is the $E\times B$ rotation frequency minus a quarter of the ion diamagnetic frequency, $f_{E\times B} - 0.25 f_{D^+}$. The yellow region is the frequency displacement between successive modes from the BES measurements across the pedestal region, i.e., mode frequency per toroidal mode number. It is found that the sum of the $E\times B$ rotation and diamagnetic frequencies is close to the observed (lab frame) mode frequency, suggesting that the modes propagate close to $V_{D^+} / 4$ in the plasma frame, where V_{D^+} is the ion diamagnetic velocity. We note that this is consistent with the frequency expected for KBM driven by the bulk ion pressure predicted from local fluid model [11]. This observation is also qualitatively similar to observations of high frequency coherent modes made in the core region of TFTR [12].

ELITE calculations [10], which are from a model based on intermediate n peeling-ballooning mode MHD stability of the tokamak edge region, have been performed and show that the discharge is not close to an ideal ballooning stability boundary. This might be due to the strong shaping of this plasma and the high-pressure gradient may put the ideal ballooning mode very deeply in the second stable regime, the design goal of the experiment. Also, the measured nonlinear decorrelation rate of these HFC modes is comparable to or exceeds the high local $E\times B$ shearing rate. These HFC modes exhibit a number of features that are qualitatively similar to characteristics predicted for KBM: n-number, poloidal mode structure, frequency separation and mode velocity. Furthermore, these modes appear in a regime where KBM is predicted to be driven unstable (high pedestal pressure gradient), hinting that these observed modes may be the KBM; at a minimum, they have KBM-like properties. To reveal the nature of the modes and have quantitative comparison with KBM theory will require more sophisticated nonlinear gyrokinetic simulations, to be examined in the future.

4. Turbulence Enhancement During RMP ELM-suppressed Plasmas

ELMs are a common feature of most quasi-steady H-mode plasmas. They are believed to occur as the pedestal pressure and current density gradients exceed thresholds associated with rapidly rising peeling-ballooning mode instabilities. Because ELMs eject a burst of hot particles on a very short time scale, they result in large transient heat fluxes, which can erode and damage first-wall materials. Thus, controlling ELMs by mitigating their size and impact or suppressing them altogether is an active research endeavor.

ELMs have been suppressed by the application of RMP to H-mode plasmas [3]. The RMP is applied via “window-frame” coils inside the vacuum vessel that produce a dominantly radial magnetic field with an n=3 toroidal mode number and a spectrum of poloidal components. When successfully applied, ELMs are suppressed for many energy confinement times (several seconds or longer) under quasi-steady plasma conditions. In addition to suppressing ELMs, application of RMP typically slows toroidal rotation, reduces density and may (but not always) adversely affect energy confinement, depending on collisionality and other discharge parameters.

The core turbulence is observed to increase dramatically, relative to that observed in an ELMing phase, as a direct consequence of RMP application to suppress ELMs. Figure 5 compares the spectra of long-wavelength density fluctuations, measured at 3 radial locations (ρ=0.68, 0.85, and 0.96) with BES, during standard ELMing H-mode operation, with that during RMP-induced ELM-suppressed operation. The inner locations show a substantial increase in fluctuation power, while the outer location (ρ=0.96) exhibits a change in spectral shape, but a less significant increase in fluctuation amplitude. In particular, the core fluctuation power increase is most dramatic for higher frequency fluctuations, with the RMP-enhanced fluctuations extending up to 400 kHz. Separate measurements show that the Doppler shift tends to decrease with RMP, so the spectral increase clearly reflects an increase in the higher wavenumber region of the low-k spectrum, since the lab-frame frequency results primarily from the *E*x*B* Doppler shift [$f_{lab} = \omega_{lab}/2\pi = (\omega_{plas} + \vec{k}\,\vec{\mathbf{v}}_{E\times B} \approx \vec{k}\,\vec{\mathbf{v}}_{E\times B})/2\pi$].

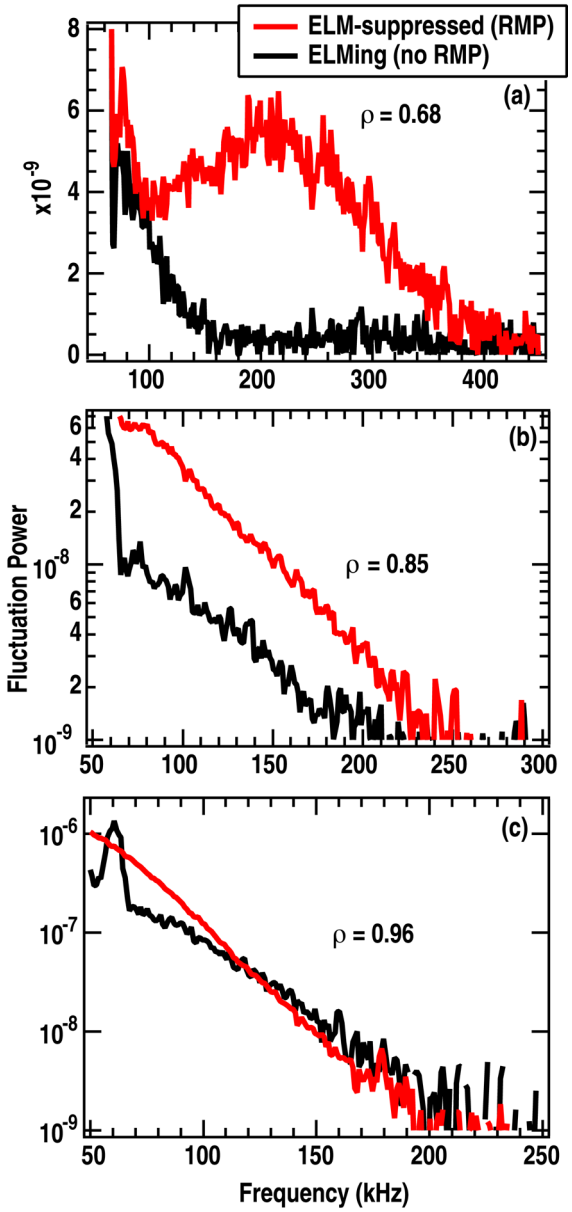

FIG. 5. Spectra of long-wavelength density fluctuations before (ELMing, black) and during RMP ELM-suppressed operation at (a) r/a=0.68, (b) r/a=0.85, (c) r/a=0.96.

The line-integrated plasma density decreases during RMP ELM-suppressed operation. A plausible hypothesis for the observed turbulence and density behavior is that the increased turbulence causes the increase in particle transport and associated density reduction. The density profile and gradient scale lengths are also found to change, potentially leading to a change in turbulent instability drive. The full explanation then likely lies in the complex and highly nonlinear dynamics of density, density gradients, turbulence, particle transport, and perhaps rotation changes with the RMP. The spatial and temporal dynamics of the core turbulence enhancement shed some light on these processes and are investigated next.

The radial profile of normalized long-wavelength density fluctuations in the ELMing phase and RMP ELM-suppressed phase are compared in Fig. 6. Broadband fluctuations are enhanced over much of the radial range $0.4 < r/a < 0.9$, with a curious null in the fluctuation enhancement near r/a=0.5. The fluctuation power spectra are integrated over approximately 70–400 kHz (the magnitude shown being the square root of integrated power) and scale with the normalized density fluctuations, $\tilde{n}/n$; overall fluctuations magnitudes are in the range $\tilde{n}/n$<1%. Of particular note, it is observed that the edge fluctuation magnitudes do not change significantly, although edge gradients do change, and ELMs are suppressed in this region. It is thought that the reduction in pressure gradients brings the plasma away from the peeling-ballooning ELM instability threshold [13]. While the turbulence spectra undergo changes with application of the RMP, density fluctuation enhancement in the edge pedestal region of

RMP ELM-suppressed plasmas does not appear to fully explain the enhanced particle transport; it appears rather that enhancement of the core ($0.75 < r/a < 0.9$) fluctuations may be the important mechanism, based on the temporal dynamics, discussed next.

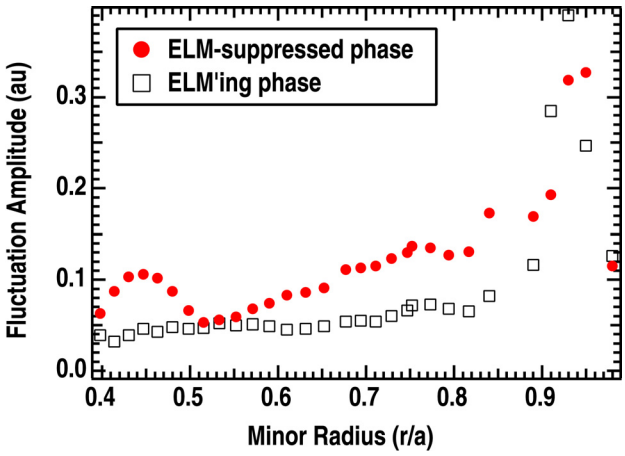

FIG. 6. Comparison of profile of normalized density fluctuation amplitude during RMP ELM-suppressed phase and ELMing phase.

The core fluctuation enhancement commences rapidly after RMP application (several milliseconds), and is further enhanced during the ELM-suppressed phase. Likewise, when the RMP is turned off, fluctuations are reduced locally within ~10 ms, before ELMs resume. This behavior suggests that the RMP causes the enhanced core turbulence that results in increased particle transport and reduced density, since the density gradients do not respond as rapidly.

To investigate the spatiotemporal dynamics of the turbulence enhancement further, a specialized experiment was conducted whereby ELMs were first suppressed via a steady RMP, and then the RMP was modulated at 5 Hz for two seconds, while the plasma stayed in an ELM-suppressed state. The coil current producing the RMP was not reduced to zero, but rather was reduced to one half; the lower value of RMP would not sustain ELM-suppression in steady-state, but does sustain ELM-free operation for the duration of the modulated time period. The relative fluctuation magnitude at three radii (r/a=0.58, 0.7, and 0.85) is shown in Fig. 7, along with the I-coil current producing the RMP field. To improve the signal-to-noise of these fluctuation measurements, the fluctuation magnitude was determined by phase locking measurements from ten periods of I-coil modulation over the two seconds for this experiment. Plasma parameters behaved in a periodic fashion over this time frame, justifying this approach. The fluctuations are resolved at 2.5 ms time resolution, with a 1 ms time step between measurements displayed. Density fluctuation spectra are evaluated for each phase-locked time period, and integrated over 80–400 kHz. It is readily apparent that the turbulence responds rapidly as the I-coil current is varied. Furthermore, the response time varies with radius. Turbulence at the outer location of r/a=0.85 responds almost immediately, essentially tracking the I-coil current on a few millisecond time scale. At the inner locations, the turbulence responds more gradually, with approximately a 20 ms response (decay) time at r/a=0.7, and up to a 40 ms decay time near r/a=0.58. These results indicate that the local turbulence responds to the applied RMP with a radially-dependent turbulence response time. Analysis of the density profile evolution shows that it modulates slightly with the I-coil current, decreasing (increasing) during the high (low) current phases. The density varies locally with an approximately 5%–10% modulation over $0.6<r/a<0.8$, though gradient variation is less. The density profile response is slower than the turbulence

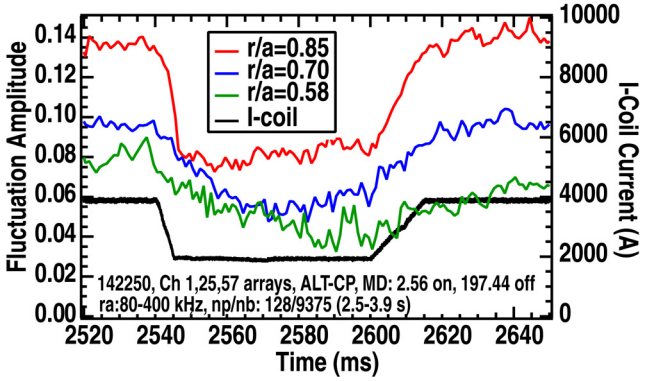

FIG. 7. Time resolved density fluctuations (phase locked measurement) at 3 radii, and modulated I-coil current.

response, suggesting that gradient changes do not explain the more rapid temporal turbulence response.

5. Summary

Turbulence dynamics in the pedestal and core region have been investigated during ELMing and ELM-free plasmas. The inter-ELM fluctuation behavior in a typical ELMing H-mode plasma exhibits a rapid increase in fluctuation power shortly after the ELM crash (few ms), as the pedestal height and gradients increase, which then saturates at a quasi-steady magnitude for upwards of 20 ms before the next ELM crash. The dual spectral bands strongly suggest that multiple instabilities coexist at the same spatial location and time. The lower-frequency band exhibits several characteristics that are qualitatively similar to predicted KBM-features, though mode identification will require more comprehensive modeling and simulations. Fluctuations in a high-pedestal pressure QH-mode plasma exhibit a set of coherent relatively high-frequency modes that, unlike the ELMing pedestal turbulence are not driven into a highly turbulent state, perhaps due to high rotational shear, but also exhibit KBM-like features. ELM-suppressed RMP discharges show that edge turbulence does not change dramatically in response to the RMP, but rather that the core turbulence increases significantly, possibly explaining the rapid density pump-out observed in these discharges. Comparison of these characteristics with models of pedestal instabilities and simulations of their nonlinear behavior will serve to help validate such simulations and further understand the highly nonlinear dynamics that limit the heights, width and gradients of H-mode pedestals.

This work was supported in part by the US Department of Energy under DE-FG02-89ER53296, DE-FG02-08ER54999, DE-FC02-04ER54698, DE-FG02-07ER54917, DE-FG02-04ER54761, and DE-AC52-07NA27344.

References

[1] SNYDER, P.B., *et al.,* Phys. Plasmas **16** (2009) 056118
[2] GROEBNER, R.J., *et al.,* Nucl. Fusion **49** (2009) 085037
[3] EVANS, T.E., *et al.,* Nucl. Fusion **45** (2005) 595
[4] McKEE, G.R., *et al.*, Plasma and Fusion Research **2** (2007) S1025
[5] BEURSKENS, M.N.A., *et al*., Phys. Plasmas Control. Fusion **51** (2009) 124051
[6] GROEBNER, R.J., *et al.,* Nucl. Fusion **50** (2010) 064002
[7] BURRELL, K.H., *et al.,* Nucl. Fusion **49** (2009) 085024
[8] GREENFIELD, C.M., *et al.,* Phys. Rev. Lett. **86** (2001) 4544
[9] SNYDER, P.B., *et al.,* Nucl. Fusion **47** (2007) 961
[10] SNYDER, P.B., *et al.,* Plasma Phys. Control. Fusion **46** (2004) A131
[11] SNYDER, P.B., PhD thesis, "Gyrofluid Theory and Simulation of Electromagnetic Turbulence and Transport in Tokamak Plasmas," Princeton University (1999).
[12] NAZIKIAN, R., *et al.,* Phys. Plasmas **3** (1996) 593
[13] OSBORNE, T.H., *et al.,* "Edge Stability of Stationary ELM-suppressed Regimes on DIII-D," J. Physics: Conf. Series **123** (2008) 012014s